

Received 9 May 2023, accepted 24 May 2023, date of publication 26 May 2023, date of current version 5 June 2023.

Digital Object Identifier 10.1109/ACCESS.2023.3280452

## RESEARCH ARTICLE

# Classical and Quantum Processing in the Deep Physical Layer

**MARCO DONALD MIGLIORE** , (Senior Member, IEEE)

Department of Electrical and Information Engineering “Maurizio Scarano” (DIEI), University of Cassino and Southern Lazio, 03043 Cassino, Italy  
ELEDIA@UniCAS, 03043 Cassino, Italy

Inter-University Research Center on the Interactions Between Electromagnetic Fields and Biosystems (IcEmB), 16145 Genoa, Italy  
National Inter-University Consortium for Telecommunications (CNIT), 43124 Parma, Italy

e-mail: mdmiglio@unicas.it

This work was supported in part by the European Union’s Horizon Europe Research and Innovation Program (NextGEM) funded by the European Union under Grant 101057527.


**ABSTRACT** The objective of this paper is to examine the processing of the electromagnetic field in the physical communication channel of wireless systems using the concept of the “Deep Physical Layer” (DPL), a layer that is positioned below the Physical Layer of the OSI model. The article delves into the fundamental concept of DPL and presents several numerical findings on devices that can process the field directly in the DPL. These devices are called Electromagnetic field Processing Devices (EPDs) and consist of reflective elements that are extensively distributed in space. They can intelligently modify the spatial configuration of the electromagnetic field to achieve efficient processing. The study reveals that EPDs offer the potential to encode a massive amount of information in the spatial domain. Additionally, the results suggest that quantum computers are an indispensable technology to gain unrestricted access to the large resources that utilizing EPDs in the DPL can unlock. To fully utilize this vast resource necessitates addressing the challenge of searching an unstructured database, which poses a difficulty for classical computers. However, this problem can be efficiently solved by quantum computers using Grover’s algorithm.

**INDEX TERMS** Communication systems, quantum computing, Grover’s algorithm, 6G, OSI model, cellular systems, MIMO systems, electromagnetic field processing, number of degrees of freedom, space-time coding.

## I. INTRODUCTION

What is the full potential of space in a wireless communication channel? And how to have full access to this potential? These are two critical questions for future communication systems, which will increasingly rely on spatial waveforms to overcome the limited availability and high cost of the radio wave spectrum. To answer these questions, we need to delve into the physics of the communication process, broaden our understanding of information, and leverage the new opportunities offered by quantum computing.

While understanding the limitations of communication systems based on the time domain is a well-established field of research that has its roots in the work of Shannon [1],

The associate editor coordinating the review of this manuscript and approving it for publication was Sandra Costanzo .

the use of space to transmit information is relatively new, and limitations associated with the space-varying waveforms are still under investigation. Analysis of information in space domain has been carried out for the first time in [2], [3], [4], [5], and [6]. The role of the Number of Degrees of Freedom of the electromagnetic field in spatial channels has been discussed from a theoretical point of view for the first time in [7], and on the base of numerical simulations in [8]. Spatial channels have been investigated in case of spherical sources in [9], [10] and [11] and in case of more general sources in [7] and [12]. The theory has been applied to analysis of ad hoc networks in [13] and [14]. Analysis of the spatial channel in terms of Kolmogorov channel capacity has been introduced for the first time in [15]. Application of the theory to antenna synthesis was proposed in [16], [17], and [18]. Recently, there is an increasing interest toward the connections between

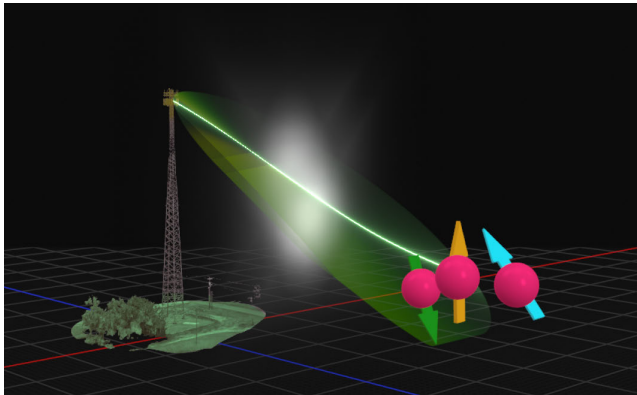


**FIGURE 1.** A pictorial view of the solution proposed to use the full potential of the DPL. Electromagnetic field Processing Devices (EPDs) act as information lenses, while quantum processing allows us to effectively decode the large amount of information made available by the EPDs.

electromagnetic and information theory, and many research groups are actively working on this topic [19], [20], [21].

As we strive to develop more efficient communication systems, we inevitably encounter restrictions imposed by the laws of physics.

In order to address these limitations, it is useful to introduce an additional layer below the Physical Layer (PL) in the OSI model. This new layer, called the Deep Physical Layer (DPL), see Fig. 2), is discussed in detail in [22]. Unlike the PL, where information is a “mathematical” quantity based on the Shannon information entropy, the DPL considers information in relation to the physics of the medium carrying the information. Specifically, in radio communications, information is determined by the number of distinguishable configurations of the electromagnetic field on the receiver. The importance of the DPL lies in the fact that the maximum amount of information that can be transmitted is determined at this level, as the performance of communication systems in terms of data throughput is governed by the laws of physics. In contrast, the “potential” offered by the DPL is expressed at the PL level depending on the specific communication strategy and technological solution.

The scheme depicted in Fig. 2 provides useful insights into enhancing communication. Firstly, it elucidates the crucial role of antennas as the sole gateway connecting the “virtual” world represented by the layers above the DPL to the “real” world of the DPL. Metaphorically, antennas transform “logical” bits into “physical bits”, which carry information according to the laws of physics. Therefore, antennas are the only means of accessing the resources present in the DPL, and, if not designed correctly, can represent the bottleneck of the telecommunication system. In this context, antennas serve as information transmission systems, whose synthesis should take into account not only conventional objectives like controlling the power density distribution but also communication-specific objectives such as channel capacity maximization. While antenna synthesis in the context of DPL

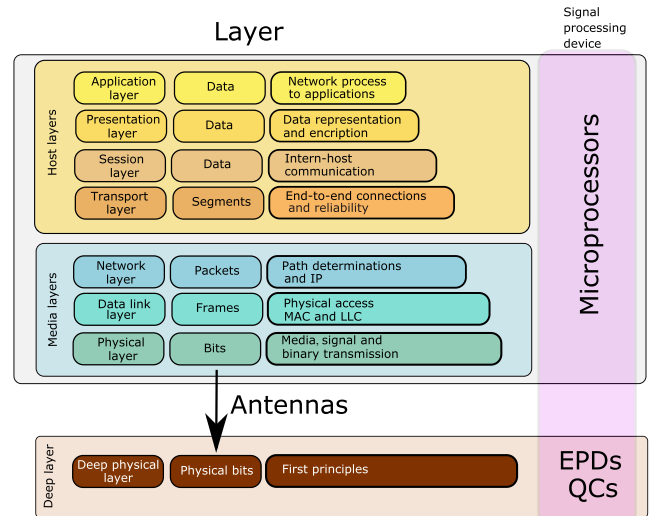


**FIGURE 2.** The OSI stack extended with The Deep Physical Layer (DPL). In the DPL, the information is associated with “states” of the electromagnetic field (i.e., field configurations at the receiver) which are distinguishable in the presence of noise. Information (i.e. field configurations) is elaborated by Electromagnetic field Processing Devices (EPDs), which operate according to classical physics, and by Quantum Computers (QCs), which operate according to quantum physics.

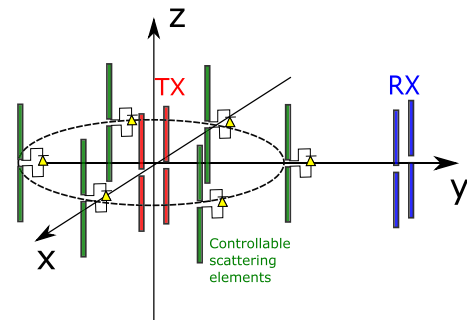


**FIGURE 3.** ADAM (ADaptive MIMO antenna) was a ‘proof of concept’ of the possibility to improve the channel capacity by controlling scattering elements in the environment, carried out at the beginning of this century [26]. In ADAM the scattering elements were placed in a circle around the TX antenna.

has been addressed in other works [16], [22], [23], this article will not delve into this topic.

A further interesting observation concerns data processing. All the layers above the DPL process the information of interest to the layer. This suggests introducing processing at the DPL level as well. However, the quantity of interest at the DPL level is the electromagnetic field, whose processing requires methodologies and devices that are profoundly different from those used in the upper layers. These devices will be called Electromagnetic field Processing Devices (EPDs) [24], [25].

The concept of EPD originates from a proof of concept called ADAM (Adaptive MIMO Antenna, [26]) developed in the early 21st century, shown in Fig. 3. ADAM generates a locally controllable environment using scattering elements connected to electronically controllable loads. The channel

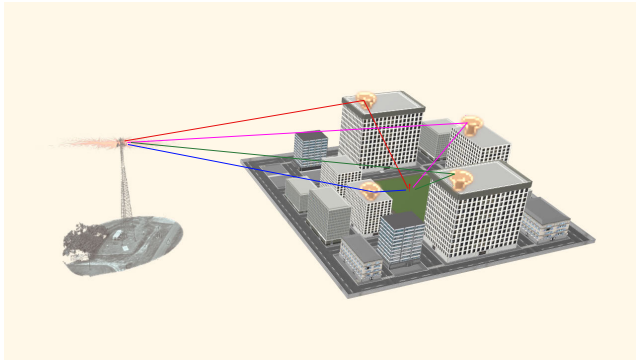


**FIGURE 4.** A pictorial view of an EPD consisting of four controllable reflecting elements. Loosely speaking, EPD can be consider an array of widely distributed scattering elements. The individual elements of an EPD can be static (no control on the reflected field), or dynamic (control on the reflected field).

operator is a function of the state of the scattering elements. By manipulating the scattering configuration of the elements, it is possible to obtain different singular value distributions of the channel operator, which optimizes the channel capacity of the MIMO system or other quantities of interest. The experimental results of a  $2 \times 2$  MIMO channel with a 30 MHz bandwidth showed a doubling of the number of spatial channel channels in the entire bandwidth [27].

EPDs can be seen as a scaled-up version of ADAM, utilizing arrays of scattering elements to achieve a degree of control over the propagation channel and improve capacity. An example of an EPD is shown in Fig. 4. Essentially, an EPD consists of an array of widely-distributed scattering elements, with individual elements that can be either static (no control on the reflected field, such as in Electromagnetic Skins (ES) [28]) or dynamic (allowing control over the reflected field, such as in Reflecting Intelligent Surfaces (RIS) [29], [30], [31], [32]). The technology behind EPDs is similar to that of ES and RIS.

More specifically, the EPDs described in this paper are static systems that are widely distributed in space. These systems are fully compatible with existing standards and can be integrated without any modifications to the communication system. It is understood that dynamic EPDs, which require the development of a specific standard, can offer even higher performance by dynamically optimizing their response.

EPDs can be thought of as “lenses” that manipulate spatial information by gathering information from large areas of space and directing it towards the receiver. This paper does not offer any specific technological solutions for EPDs, but instead provides a high-level analysis of electromagnetic field processing. Therefore, similar to [22], this paper presents a framework for examining and comprehending electromagnetic field processing at a fundamental level, prior to introducing the specific details of the EPD used in the elaboration. This enables a “bird’s eye view” of the field elaboration process.

Based on the analysis conducted in this study, it appears that utilizing EPDs in the DPL could allow for encoding a significant amount of data in the spatial domain. However, to make these extensive resources available to higher OSI layers, the challenge of searching an unstructured database must be addressed. This task is difficult to accomplish with classical computers, but quantum computers have the potential to efficiently solve this problem. This implies that quantum computers may be a crucial enabling technology for gaining unrestricted access to the vast resources that the use of EPDs in the DPL can offer.

It should be emphasized that the approach taken in this paper is quite distinct from the methods employed in the field of quantum communication research. Quantum communication utilizes the principles of quantum mechanics to achieve secure communication. Examples of this include quantum key distribution (QKD), quantum teleportation, and quantum networks [33]. In all of these applications, as well as in quantum sensing, which involves using quantum systems to detect and measure various physical properties, quantum signal generation, transmission, and reception are critical topics.

This paper does not rely on quantum phenomena for communication and detection, which instead are based on classical physics, and do not involve entanglement in the communication process. Instead, quantum phenomena are utilized to speed up codeword decoding with the help of quantum computers.

The field of quantum computing offers numerous hardware solutions, including superconducting qubits, trapped ion qubits, and photonic qubits, each with its own strengths and weaknesses [34]. Scientists are actively working to address the challenges associated with each approach. Alongside the advancement of quantum computer hardware, various programming languages have been developed [35] and are currently accessible.

One of the most popular programming languages for quantum computing is Qiskit [36], which allows developers to build quantum circuits and execute them not only on simulators but also on IBM’s quantum hardware. A very simple example using Qiskit is reported in the Appendix showing the ‘logic’ of the quantum computing programming. However, many other languages for quantum computing are available, as Cirq developed by Google, Q# by Microsoft and PyQuil by Rigetti Computing.

As noted at the beginning of this Section, the goal of this paper is to identify a strategy to use the full potential offered by the DPL in terms of spatial information. The level of enhancement achieved is determined by various factors, such as antenna design, frequency, propagation environment, and the EPD’s overall design, and it can theoretically exceed 100 bits per symbol. The quantity of information is so vast that even methods that do not utilize the entire capability of the DPL may be deemed acceptable. Depending on the extent to which this potential is wasted, suboptimal techniques may be utilized, such as scaling the decoding problem to a point where it can be handled by classical computers.

**TABLE 1.** Symbols used in the classical physics portion of the DPL communication process.

	classical physics
$ v_h\rangle$	$h$ -th singular function of the current
$ u_h\rangle$	$h$ -th singular function of the field
$\sigma_k$	$h$ -th singular value of $\mathbf{A}$
$ e\rangle$	field state
$ c\rangle$	current distribution state
$\lambda$	wavelength in free space
$\mathcal{A}$	TX $\rightarrow$ RX radiation operator
$\mathcal{B}$	TX $\rightarrow$ EPD radiation operator
$\mathcal{C}$	EPD $\rightarrow$ RX radiation operator
$\mathcal{W}$	EPD scattering operator
$(\sigma_h,  u_h\rangle,  v_h\rangle)$	singular system of $\mathcal{A}$
$(\Sigma_{\mathcal{A}}, \mathcal{U}_{\mathcal{A}}^l, \mathcal{U}_{\mathcal{A}}^r)$	singular system of $\mathcal{A}$
$(\Sigma_{\mathcal{B}}, \mathcal{U}_{\mathcal{B}}^l, \mathcal{U}_{\mathcal{B}}^r)$	singular system of $\mathcal{B}$
$(\Sigma_{\mathcal{C}}, \mathcal{U}_{\mathcal{C}}^l, \mathcal{U}_{\mathcal{C}}^r)$	singular system of $\mathcal{C}$
$(\Sigma_{\mathcal{W}}, \mathcal{U}_{\mathcal{W}}^l, \mathcal{U}_{\mathcal{W}}^r)$	singular system of $\mathcal{W}$
$C_\epsilon$	$\epsilon$ -capacity
$\dagger$	adjoint of an operator

**TABLE 2.** Symbols used in the quantum physics portion of the DPL communication process.

	quantum physics
$ x_h\rangle$	$h$ -th quantum eigenstate
$ x_k\rangle$	target eigenstate
$ s\rangle$	quantum state
$G$	Grover operator
$U_{x_k}$	Grover oracle
$U_s$	Diffusion operator
$\lambda_k$	Eigenvalues of the $k$ -th eigenstate

The paper is structured as follows. Section II introduces a reformulation of the DPL theory using bra-ket symbols commonly used in quantum physics. This section aims to prevent confusion with symbols used in the quantum section by modifying some of the symbols used in [22].

In Section III, the classical computing aspect is discussed, while Section IV presents quantum computing.

Section V provides an example that illustrates the potential and challenges of fully utilizing the DPL’s resources for upper layers.

Section VI presents the conclusions.

Finally, in the Appendix, a simple implementation of Grover’s algorithm using Qiskit language is provided, which can be executed on IBM quantum computers.

## II. INFORMATION IN THE DEEP PHYSICAL LAYER

Suppose Alice wants to convey a message to Bob. Before the connection, Alice and Bob prepare a codebook containing a series of code words. During the communication process, Alice sends a specific code word. The goal of the communication is to identify the code word transmitted by Alice even in a noisy communication channel.

In the Deep Physical Layer (DPL), all stages of the communication process are closely linked to the physics of the information transmission [22]. The transmitter is modeled as electric current densities that radiate in the environment,

while the receiver is simply an observer that identifies the configuration of the electromagnetic field on an observation manifold  $\mathcal{M}$ . The specific field configuration on the observation manifold will be called the ‘state’ of the received field.

The codebook consists of unique code words that are encoded in distinct states of the received field. To receive the message, the receiver must determine the exact state of the received field even if corrupted by noise or measurement errors during the reception phase. The maximum number of states that the receiver can *distinguish* in the presence of noise establishes the upper limit of reliable information transmission that the system can accomplish.

As noted in the Introduction, in this paper, we will focus on the use of the space to transmit information. In particular, we will consider the ‘pure spatial communication system’ model introduced in [7], i.e., a harmonic communication system that uses only spatial resources to transmit information. This allows isolate the contribution of the space domain from the contribution of the time domain in the communication. Moving forward, we will omit the time dependence notation  $e^{j\omega t}$  (where  $\omega$  represents the angular frequency of currents and fields) in our discussions.

With reference to Fig. 5, let us consider a proper basis<sup>1</sup>  $\{|v_0\rangle, |v_1\rangle, \dots\}$  in an infinite dimensional separable Hilbert space equipped with  $L_2$  norm and let us represent the current distribution  $|c\rangle$  on the radiating systems using this basis [37]:

$$|c\rangle = \sum_{h=1}^{\infty} |v_h\rangle \langle v_h|c\rangle \tag{1}$$

The set of all the possible current distributions on the radiating system will be called  $X$ . We will suppose that  $X$  is bounded, and its radius is finite, f.i. equal to one.<sup>2</sup> The specific current distribution  $|c\rangle$  will be called a ‘state’ of current distribution. Any state is a superposition of the basis functions  $|v_h\rangle$ .

The field radiated by the current is observed on the observation manifold  $\mathcal{M}$ . We introduce a proper basis<sup>3</sup>  $\{|u_0\rangle, |u_1\rangle, \dots\}$  in an infinite dimensional separable Hilbert space equipped with  $L_2$  norm. The observed field  $|e\rangle$  is represented by superposition of the basis functions [37]:

$$|e\rangle = \sum_{h=1}^{\infty} |u_h\rangle \langle u_h|e\rangle \tag{2}$$

The set of all the received field configurations on  $\mathcal{M}$  will be called  $Y$ , while  $|e\rangle$  represents the ‘state’ of field configuration on the observation manifold.

The operator  $\mathcal{A}$ , called ‘radiation operator’ [38], maps elements of  $X$  into elements of  $Y$  [38] (Fig. 6(a)):

$$|e\rangle = \mathcal{A} |c\rangle \tag{3}$$

<sup>1</sup>The  $\{|v_h\rangle\}$  basis will be specified after introducing the radiation operator.

<sup>2</sup>This constraint limits the energy of the currents on the antennas [7].

<sup>3</sup>The  $\{|u_h\rangle\}$  basis will be specified after introducing the radiation operator.



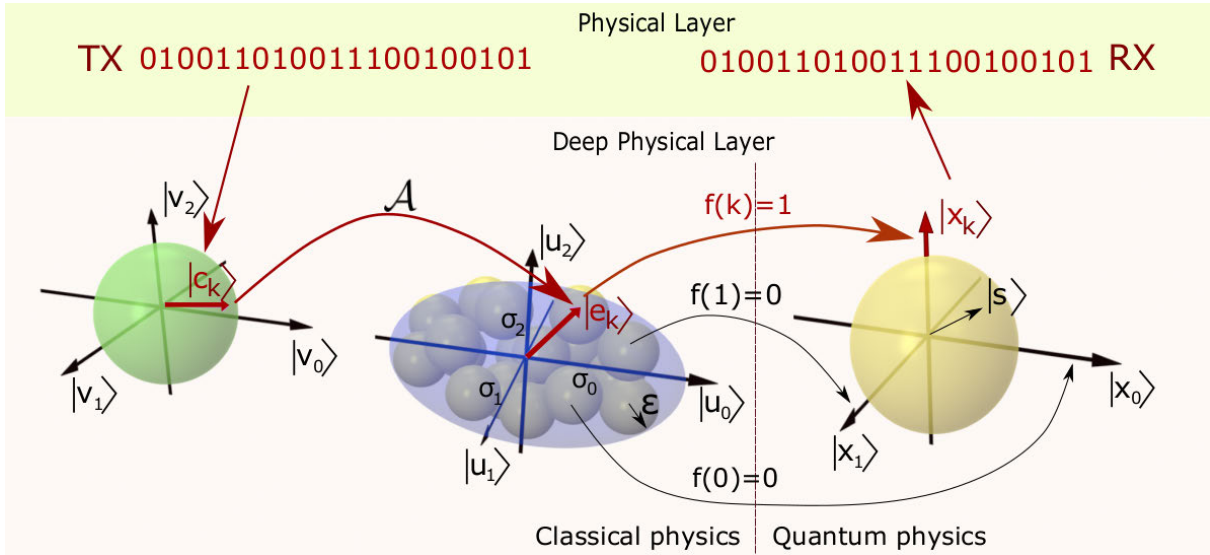


**FIGURE 5.** The communication process in the DPL. The  $k$ -th codeword is associated with the  $|c_k\rangle$  state of the current distributions on the transmitting antenna. The radiation operator  $\mathcal{A}$  maps  $|c_k\rangle$  into the state  $|e_k\rangle$  of the field on the receiving antenna. Due to the presence of noise and measurement uncertainty, the measured state is different, but in any case is inside  $k$ -th  $\epsilon$ -sphere of uncertainty. The oracle flips the quantum eigenstate  $|x_k\rangle$  associated to the  $k$ -th  $\epsilon$ -sphere, and the Grover algorithm is iteratively applied to the quantum system. When the probability that the state of the quantum system collapses in  $|x_k\rangle$  becomes one, measurement on the system is carried out, and the  $\epsilon$ -sphere to which  $|x_k\rangle$  belongs is identified.

$\mathcal{A}$  is an integral operator whose Kernel is given by the Green's function [15], [39], which takes into account the physical mechanism of electromagnetic propagation.

Since  $\mathcal{A}$  is a completely continuous (also called compact) operator [37], [39], it admits the Hilbert-Schmidt representation in terms of singular system,  $(\sigma_h, |u_h\rangle, |v_h\rangle)$  wherein  $\sigma_1 \geq \sigma_2 \geq \dots \geq \sigma_n \geq \dots$  are the singular values of the operator and  $|u_h\rangle, |v_h\rangle$  are called singular functions. [15], [37]. The singular values are real, are listed in decreasing order ( $\sigma_{h+1} \leq \sigma_h$ ) and  $\lim_{h \rightarrow \infty} \sigma_h = 0$  [37], [39]. In the following, the basis functions  $|v_k\rangle$  will be called the singular functions of the current distribution, while the basis functions  $|u_k\rangle$  will be called the singular functions of the electric field on  $\mathcal{M}$ .

The Hilbert-Schmidt expansion [37] diagonalizes the operator obtaining [7], [39]:

$$|e\rangle = \mathcal{A}|c\rangle = \sum_{h=1}^{\infty} \sigma_h |u_h\rangle \langle v_h|c\rangle \quad (4)$$

or equivalently [39]:

$$\mathcal{A} = \mathcal{U}'_{\mathcal{A}} \Sigma_{\mathcal{A}} \mathcal{U}''_{\mathcal{A}}{}^{\dagger} \quad (5)$$

wherein  $\mathcal{U}'_{\mathcal{A}}$  and  $\mathcal{U}''_{\mathcal{A}}$  are unitary operators,  $\Sigma_{\mathcal{A}}$  is a diagonal operator that scales the components of  $\mathcal{U}''_{\mathcal{A}}|c\rangle$  according to the singular values of  $\mathcal{A}$ , and the superscript  $\dagger$  stands for the Hermitian conjugate (or adjoint) of the operator.

In practical cases, observation of an the elements in  $Y$  is unavoidably affected by noise and uncertainty, which limit the number of states that can carry information. We consider

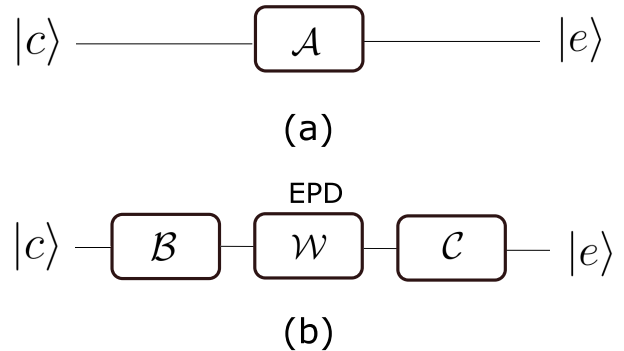


**FIGURE 6.** (a) Functional scheme of the TX-RX radiation operator; (b) Functional scheme of the TX-RX radiation operator in case of presence of EPD.

indistinguishable two elements of  $Y$  having a distance smaller than a given quantity, let  $\epsilon$  be [15]. The quantity  $\epsilon$  depends on the noise and on accuracy of our measurement system.

Let us now consider an  $\epsilon$ -packing of  $Y$ , i.e., a family of not intersecting open balls with centers in  $Y$  and radius  $\epsilon$  (called  $\epsilon$ -balls, Fig. 5). Since  $Y$  is totally bounded [22], it admits a finite  $\epsilon$ -packing for any  $\epsilon > 0$  [16], [22], [37].

The supremum of the number of balls of all the possible  $\epsilon$ -packing of  $Y$ , let  $P_{\epsilon}$  be, is called *packing number* [40].

The Kolmogorov  $\epsilon$ -capacity of  $Y$ , let  $C_{\epsilon}$ , is<sup>4</sup> [40]:

$$C_{\epsilon} = \log_2(P_{\epsilon}) \quad (6)$$

<sup>4</sup>In many papers the capacity is indicated as  $C_{2\epsilon}$ . We will denote it as  $C_{\epsilon}$  for sake of notation simplicity.

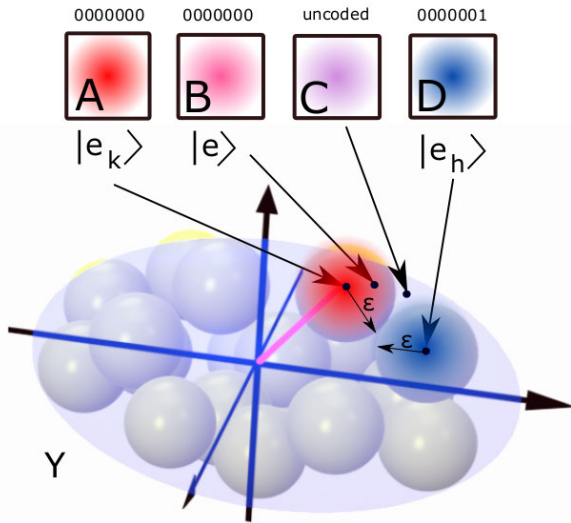


**FIGURE 7.** Each field configuration on the observation domain  $\mathcal{M}$  is associated to a functional point in the set  $Y$ ; A,B,C,D are 4 different field configurations on  $\mathcal{M}$ . The measured field is affected by noise that prevents to reliably distinguish two field distributions associated to points closer to  $\epsilon$ . Let's suppose that the noiseless received field is the A field distribution ( $|e_k\rangle$ ), decoded for example as '000000' bit string. Due to the noise the received field is B ( $|e\rangle$ ) instead of A. In presence of an  $\epsilon$  noise level B can fall in any point at distant not larger than  $\epsilon$ . All the field configurations falling inside the sphere of radius  $\epsilon$  centered in  $|e\rangle_k$  are decoded as  $|e\rangle_k$ , i.e. as '000000' bit string. All the field configurations that do not belong to the set of  $\epsilon$ -spheres are not used to encode information to avoid ambiguity. Consequently, the maximum number of information is equal to the maximum number of distinguishable field configurations (i.e. 'states' of the received field) in presence of noise.

and turns out to be [41]:

$$\sum_{h=1}^{NDF_\epsilon} \log_2 \left( \frac{\sigma_h}{2\epsilon} \right) < C_\epsilon \leq \sum_{h=1}^{NDF_\epsilon} \log_2 \left( \frac{2\sqrt{2}\sigma_h}{\epsilon} \right) \quad (7)$$

The number  $NDF_\epsilon$  is the effective dimension of the set  $Y$ . In presence of an  $\epsilon$  level of uncertainty it is possible to truncate the series (4) to the first  $NDF_\epsilon$  terms [15], obtaining [7]:

$$|e\rangle = \mathcal{A} |c\rangle = \sum_{h=1}^{NDF_\epsilon} \sigma_h |u_h\rangle \langle v_h|c\rangle \quad (8)$$

The value of  $NDF_\epsilon$  is equal to the number of singular values above the noise level  $\epsilon$ , and is called the *Number of Degrees of Freedom of the field* at the  $\epsilon$  level ( $NDF_\epsilon$ ) [16]. The  $NDF_\epsilon$  is solution of a sphere-packing problem and is strictly related to the Number of Degrees of Freedom of the field introduced by Bucci and co-worker [42], that, however, is related to sphere-covering problems arising in approximation theory [40], [43]. Indeed, in the case of far-field condition and free space propagation, the  $NDF_\epsilon$  is practically equal to the Number of Degrees of Freedom defined by Bucci in the framework of field approximation.<sup>5</sup>

Summarizing, the field  $|c\rangle$  on  $\mathcal{M}$  can be represented as superpositions of the singular functions  $|u_k\rangle$ . However, only

<sup>5</sup>The  $NDF_\epsilon$  turns out to be only one unit smaller than the Number of Degrees of Freedom defined in the framework of field approximation.

$C_\epsilon$  states are distinguishable in the presence of an  $\epsilon$ -level noise and can carry distinguishable codewords. Accordingly, the system can handle a 'codebook' with a number of codewords up to  $N = 2^{C_\epsilon}$ . Each codeword is associated with a different ball of an optimal (i.e. containing the maximum number of non intersecting balls)  $\epsilon$ -packing of the set of the received field configurations:

$$\begin{aligned} \text{codeword}_0 &\rightarrow |e_0\rangle = \mathcal{A} |c_0\rangle \\ \text{codeword}_1 &\rightarrow |e_1\rangle = \mathcal{A} |c_1\rangle \\ &\dots \\ \text{codeword}_h &\rightarrow |e_h\rangle = \mathcal{A} |c_h\rangle \\ &\dots \\ \text{codeword}_{N-1} &\rightarrow |e_{N-1}\rangle = \mathcal{A} |c_{N-1}\rangle \end{aligned} \quad (9)$$

wherein  $|e_h\rangle$  is the center of the  $h$ -th sphere. The field configuration  $|e\rangle_k$  represents a 'physical symbol' encoding  $C_\epsilon$  bits (see Fig. 7).

The determination of  $C_\epsilon$  and consequently the number of bits assigned to each state is dependent on the level of noise and the propagation channel. Prior to transmission, its value must be established through channel sounding.

Let us suppose that Alice sends the  $k$ -th codeword, see Fig. 5. The transmitter selects the  $|c_k\rangle$  state of the current distribution, which gives the  $|e_k\rangle$  state of the field on  $\mathcal{M}$  in the absence of noise. Due to the noise, the state of the received field is different, f.i.  $|e\rangle$ . However, this state belongs to the same  $k$ -th ball to which  $|e_k\rangle$  belongs. Consequently, the receiver must identify the ball to which the  $|e\rangle$  state belongs. To identify the ball, we introduce the following Boolean function  $f(h)$ :

$$f(h) = \begin{cases} 1 & \text{if } |\langle e_h|e\rangle|^2 < \epsilon^2 \\ 0 & \text{if } |\langle e_h|e\rangle|^2 > \epsilon^2 \end{cases} \quad (10)$$

The condition,  $f(k) = 1$  identifies the ball containing the transmitted signal as the  $k$ -ball.

The resources potentially available in the DPL can be huge, and the number of codewords that can be encoded in the spatial domain can quickly reach several million, even in the case of small arrays.

To give a more concrete idea of the potentialities present in the DPL, we consider the specification of an actual FR2 5G system currently in service described in [44]. The system works in 27.1 – 27.3 GHz band and uses  $\mu = 3$  numerology, i.e. 112000 symbols per second and 1667 subcarriers. Taking into account that only the 75% is available for downlink connection, almost 150 millions of Resource Elements (REs) are available in downlink. Supposing that all the REs encode 8 bits (the maximum possible in 5G standard) we have almost 1.2 Gb/s.

Let us now consider all the potential available in the DPL. As noted earlier, in this case  $NDF_\epsilon$  is almost equal to the Number of Degrees of Freedom defined in [43], which turns out to be  $\simeq 4\text{Area}/\lambda^2$  where Area is the area of the radiant

system and  $\lambda$  is the wavelength. Suppose the system uses a square antennas of  $\ell \times \ell$  area, where  $\ell$  is the side length of the antennas. A rough evaluation of the order of magnitude of the  $\epsilon$ -capacity can be obtained by the following formula [15]:

$$C_\epsilon \simeq \left(\frac{2\ell}{\lambda}\right)^2 \log_2 \left(\frac{2\sigma}{\epsilon}\right) \quad (11)$$

wherein all the relevant singular values have been supposed equal for simplicity.

In case of  $\ell=0.5$  m and  $2\sigma/\epsilon = 10$  the  $\epsilon$ -capacity turns out to be greater than  $2.5 \cdot 10^4$  bits. If the full potential of space coding is used in the 5G frame, the bit rate increases to  $\simeq 3.7$  Tb/s, reaching the goal expected in 6G systems.

However, the above example is quite optimistic. Indeed, two main problems limit the amount of information that can be encoded in actual conditions using the spatial domain.

First, the number of degrees of freedom  $NDF_\epsilon$  we obtain on the observation surface  $\mathcal{M}$  depends on the propagation environment. In some cases, the  $NDF_\epsilon$  may decrease to only one or zero (no communication) depending on the specific environment, completely losing all the potential present in the DPL.

Furthermore, identifying the received codeword in a set  $Y$  containing millions of balls is a great challenge. The position of the balls in an optimal packing is almost random, and fully exploiting the great potential present in the DPL requires an effective search method on  $Y$  sets containing millions of  $\epsilon$ -spheres. Consequently, the receiver must search in a large unsorted set of data. This requires  $O(2^{C_\epsilon})$  queries using computers based on ‘classical’ physics, limiting the number of balls that can be used to encode information and wasting a large amount of potential resources.

The above two problems will be discussed in more detail in the following two sections.

### III. CLASSICAL PROCESSING IN THE DPL

As noted in the previous Section, the radiation operator  $\mathcal{A}$  can be represented as  $\mathcal{A} = \mathcal{U}_A^l \Sigma_A \mathcal{U}_A^{r\dagger}$ , wherein  $\mathcal{U}_A^l$  and  $\mathcal{U}_A^r$  are unitary operators whose effects, from a geometrical functional point of view, are simple rotations, while  $\Sigma_A$  is a diagonal operator that scales the components of  $\mathcal{U}_A^r |c\rangle$  according to the singular values of  $\mathcal{A}$ .

Consequently, the  $\mathcal{A}$  radiation operator maps the unit  $L_2$ -norm ball  $X$  into a compact hyper ellipsoid  $Y$ , whose  $n$ -th semi-axis length is equal to the  $n$ -th singular value of the  $\mathcal{A}$  operator. Hence, the shape of  $Y$  is fixed by the  $\Sigma_A$ , i.e., by the singular values of  $\mathcal{A}$ , while the other operators only make base changes. Since the  $\epsilon$ -capacity depends on the shape of  $Y$ , a natural question is whether it is possible to modify the geometry of  $Y$  to increase the capacity.

This is indeed possible by modifying the radiation operator using specific devices, that will be called *Electromagnetic field Processing Devices* (EPDs) [24].

We suppose that the EPD performs a linear transformation of the incident field<sup>6</sup> and admits the following model [39]:

$$\mathcal{W} = \mathcal{U}_W^l \Sigma_W \mathcal{U}_W^{r\dagger} \quad (12)$$

wherein  $\{\mathcal{U}_W^l, \mathcal{U}_W^r, \Sigma_W\}$  is the singular system of  $\mathcal{W}$ . We suppose that the operator is compact, as happens in any physically realizable device [22].

The propagation between the transmitting source and the receiving surface of the EPD is modeled by the linear radiation operator [39]:

$$\mathcal{B} = \mathcal{U}_B^l \Sigma_B \mathcal{U}_B^{r\dagger} \quad (13)$$

wherein  $\{\mathcal{U}_B^l, \mathcal{U}_B^r, \Sigma_B\}$  is the singular system of  $\mathcal{B}$ . In the following the set  $\mathcal{B} |c\rangle$  will be called  $Y_B$ .

The EPD radiates acting as a source. The propagation between the EPD and  $\mathcal{M}$  is modeled by the radiation operator [39]:

$$\mathcal{C} = \mathcal{U}_C^l \Sigma_C \mathcal{A}_C^{r\dagger} \quad (14)$$

wherein  $\{\mathcal{U}_C^l, \mathcal{U}_C^r, \Sigma_C\}$  is the singular system of  $\mathcal{C}$ . The set of the outputs of  $\mathcal{C}$  will be called  $Y_C$ .

The communication channel from the source to  $\mathcal{M}$  is modeled by the linear operator  $\mathcal{A} = \mathcal{B}\mathcal{W}\mathcal{C}$  (Fig. 6(b)) that can be written as:

$$\mathcal{A} = \mathcal{U}_B^l \Sigma_B \mathcal{U}_B^{r\dagger} \mathcal{U}_W^l \Sigma_W \mathcal{U}_W^{r\dagger} \mathcal{U}_C^l \Sigma_C \mathcal{U}_C^{r\dagger} \quad (15)$$

wherein  $\mathcal{U}_B^{r\dagger} \mathcal{U}_W^l$  and  $\mathcal{U}_W^{r\dagger} \mathcal{U}_C^l$  act rotations.<sup>7</sup> Consequently, it is generally possible to modify the geometry of  $Y$  and the  $\epsilon$ -capacity by adequately choosing the electromagnetic response of the EPD.

From a ‘‘geometrical’’ perspective, the effect of the EPDs is a modification of the shape of the  $Y$  set, increasing  $C_\epsilon$ .

A first way to modify the shape increasing the capacity is to maximize the length of the main axis of the hyper ellipsoid. This is the solution generally adopted in RISs (Reflecting Intelligent Surfaces) [45], whose main application is to extend the wireless connection in Non Line of Sight propagation environment. However, this solution is optimal only if only one spatial channel is available.

A different approach is to maximize the volume of  $Y$  increasing the number of spatial communication subchannels, i.e., of the effective dimensions of the  $Y$  hyper ellipsoid [26]. In this paper we will focus our attention on this solution using transmitting surfaces [24] that act as ‘lenses’ for information.

### IV. QUANTUM PROCESSING USING GROVER’S ALGORITHM

The discussion in the previous Section shows the great potentiality present in the DPL. However, taking advantage of such potentiality is not straightforward since the receiver must

<sup>6</sup>In this paper, we do not consider nonlinear field elaboration, even if this does not exclude the possibility of building EPDs performing some nonlinear field processing.

<sup>7</sup>Note that  $X_C$  is generally a compact hyperellipsoid whose shape depends on  $\mathcal{B}$  and  $\mathcal{W}$ , while  $Y_C$  is equal to the set  $Y$  of  $\mathcal{A}$ .

search in a large unsorted data set. As previously noted, this limits the number of balls that can be used to encode information.

A possible solution to overcome this problem is to use quantum computation. In particular, the use of Grover's Quantum Search Algorithm (GQSA) [46], [47] is proposed. GQSA finds the desired entry with 100% probability of success with only  $O(\sqrt{N})$  queries [48], wherein  $N$  is the number of items in the database. This makes it possible to handle large  $\epsilon$ -packing sets.

In quantum computing, information is manipulated taking advantage of some quantum phenomena that do not have equivalent in the classical physics, such as quantum wave function superposition and entanglement.

Let us suppose that the number of  $\epsilon$ -spheres in an optimal  $\epsilon$ -sphere-packing (i.e. with maximum number of  $\epsilon$ -sphere) is  $N = 2^n$ , and consider a quantum system and an observable having  $N$  eigenstates. Let  $x_h$  be the  $h$ -th eigenstates, and  $\lambda_h$  the relative eigenvalue, assumed to be known.

We associate the  $h$ -th eigenstate  $x_h$  to the  $\epsilon$ -sphere having center element  $|e_h\rangle$ . Consequently, we have a one-to-one association between the  $\epsilon$ -spheres and the eigenstates. Identification of a specific  $\epsilon$ -sphere requires to measure the eigenvalue of the eigenstate associated to the  $\epsilon$ -sphere (Fig. 5)

Now, let us suppose that the received signal belongs to the  $k$ -th  $\epsilon$ -sphere. Accordingly, the Boolean function in Eq. 10 gives  $f(h) = 1$  for  $h = k$ , indicating  $|x_k\rangle$  as goal state, or, in other word, the output of the measurement of the observable must be  $\lambda_k$ . However, in the measurement process the wave function collapses in a random eigenstate. Shortly, the key of quantum computation is to force the system to evolve so that the state has a high probability of collapsing into the eigenstate solution of the problem of our interest (i.e., into the  $k$ -th eigenstate in our example).

To obtain this controlled dynamical evolution of the system, as a preliminary step, the Grover's procedure poses the wavefunction in a uniform superposition of eigenstates [33]:

$$|s\rangle = \frac{1}{\sqrt{N}} \sum_{h=0}^{N-1} |x_h\rangle \quad (16)$$

Let us introduce  $|x_k^\perp\rangle$  [33]:

$$|x_k^\perp\rangle = \frac{1}{\sqrt{N-1}} \sum_{h=0, h \neq k}^{2^n-1} |x_h\rangle \quad (17)$$

that spans the hyperspace orthogonal to the 'goal' state  $|x_k\rangle$ , i.e.  $\langle x_k^\perp | x_k \rangle = 0$ .

To obtain an intuitive geometrical approach, it is useful to discuss the effect of the different operators involved in the Grover's algorithm on the  $|x_k^\perp\rangle$ - $|x_k\rangle$  plane (see Fig. 8). On this plane, the state  $|s\rangle$  can be represented as  $|s\rangle = \sin(\theta/2) |x_k\rangle + \cos(\theta/2) |x_k^\perp\rangle$  (Fig. 8(a)). The probability that  $|s\rangle$  collapses in  $|x_k\rangle$  is equal to the square of the projection of  $|s\rangle$  on  $|x_k\rangle$ , i.e.  $1/N$ . For large  $N$  the angle  $\theta/2$  can be approximated as  $\theta/2 \simeq 1/\sqrt{N}$ .

To increase the probability that the quantum system collapses in  $|x_k\rangle$ , the GQDS exploits the amplitude amplification strategy [49].

As first step, GQDS introduces the operator  $U_{x_k}$  called oracle [33]:

$$U_{x_k} = I - 2 |x_k\rangle \langle x_k| \quad (18)$$

that changes the sign of the amplitude of  $|x_k\rangle$  [33]:

$$\begin{aligned} |\psi\rangle = U_{x_k} |s\rangle &= \\ &= \frac{1}{\sqrt{N}} \sum_{h=0, h \neq k}^{N-1} |x_h\rangle - \frac{1}{\sqrt{N}} |x_k\rangle \end{aligned} \quad (19)$$

The oracle rotates  $|s\rangle$  in the  $|x_k^\perp\rangle$ - $|x_k\rangle$  plane by an angle  $-\theta$ , wherein the minus sign denotes a clockwise rotation direction (Fig. 8(b)).

In practice, the oracle reflects  $|\psi\rangle$  over  $|x_k^\perp\rangle$ . The projection of  $|\psi\rangle$  on  $|x_k\rangle$  is  $\simeq -1/\sqrt{N}$  and hence the probability that  $|s\rangle$  collapses in  $|x_k\rangle$  is still  $1/N$ .

In order to increase this probability, a further unitary operator  $U_s$ , called diffusion operator, is applied [33]:

$$U_s = 2 |s\rangle \langle s| - I \quad (20)$$

that rotates  $|\psi\rangle$  by  $+2\theta$  in anti-clockwise direction (Fig. 8(c)).

The operator acting these two rotations is called the Grover operator  $G$ :

$$G = U_s U_{x_k} \quad (21)$$

The Grover operator is repeatedly applied  $r$  times until the state  $|\psi_r\rangle = G^r |s\rangle$  becomes parallel to  $|x_k\rangle$ , where  $G^r$  represents the application of the  $G$  operator  $r$  times.

Imposing

$$\frac{\theta}{2} + r\theta = \frac{\pi}{2} \quad (22)$$

we obtaining a value of  $r \simeq \frac{\pi}{4} \sqrt{N}$  iterations.

Accordingly, after  $O(\sqrt{N})$  iterations, the probability that  $|\psi^r\rangle$  collapses in the goal eigenstate is almost one.

## V. NUMERICAL EXAMPLES

Antennas are one of the few devices that cannot be miniaturized: the higher the performance required in terms of beam size, the larger the electrical dimensions of the antennas. While small antennas are desirable, the current technology is forced to use larger and larger antennas to reach higher bit rates [50].

The analysis carried out in the previous sections of this paper suggests that EPDs allow for a considerable increase in the bit rate. It is, therefore, interesting to investigate the performances obtainable using small antennas when EPDs are used.

As an example, let us consider (see Fig.9) a TX antenna (blue square in the figure) and an RX antenna (black square in the figure) consisting of small planar radiating/receiving



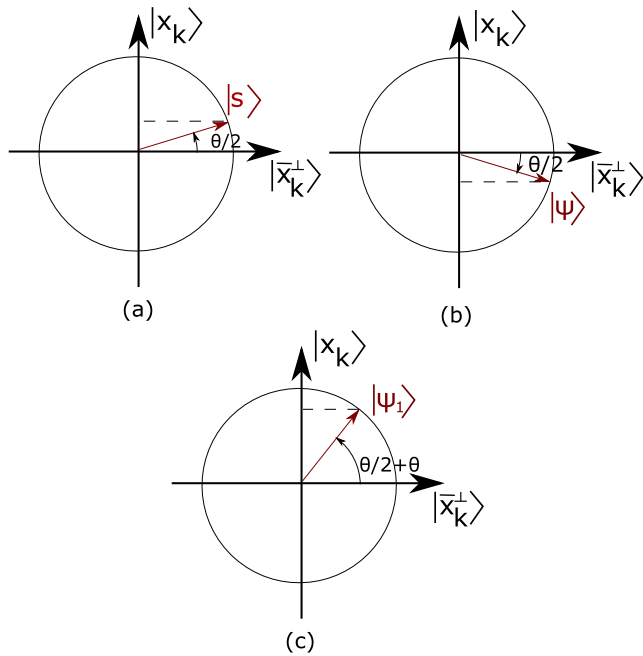


**FIGURE 8.** a): at the beginning of the Grover's procedure, the quantum system's state is a uniform superposition of the  $N$  eigenstates (in the example  $N = 4$ ), each of which is associated with a different  $\epsilon$ -sphere of  $Y$ ; the  $|x_k\rangle$  eigenstate associated with the sphere containing the received signal is the 'goal' state; the probability that the state collapses in the "target" state in the measurement process is  $1/N$ . (b): the oracle flips  $|x_k\rangle$ . The probability that the system state collapses in the "target" state is still  $1/N$ . (c): the scattering operator rotates the state vector obtaining "amplitude amplification," increasing the probability that the system state collapses in the "target" state in the measurement process. Each time the procedure repeats, the state of the system rotates by  $\theta$ .

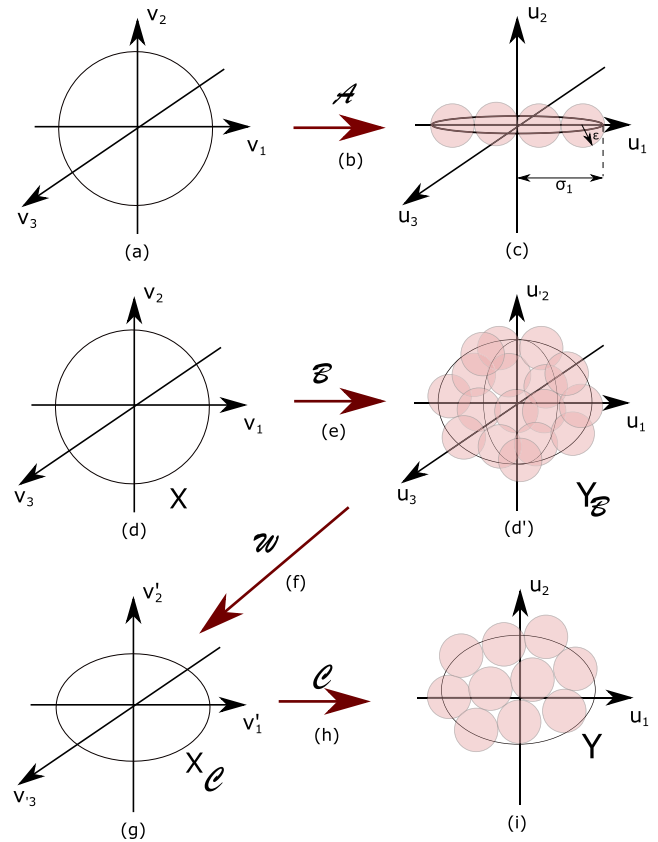


**FIGURE 10.** In the absence of an EPD device, the radiation operator  $\mathcal{A}$  (labeled as b) maps the set  $X$  of currents (marked as a) in a highly elongated hyper ellipsoid (labeled as c). In the presence of EPD, the radiation operator  $\mathcal{B}$  (labeled as e) maps the set of currents on the antenna ( $X$ , labeled as d) into a large hyper ellipsoid  $Y_B$  (labeled as f). The received field excites a current distribution on the EPD, that is controlled by the operator  $\mathcal{W}$  (step f). The radiation operator  $\mathcal{C}$  (labeled as h) maps the set  $X_C$  of currents on the EPD (labeled as g) into a large hyper ellipsoid  $Y$  (labeled as i). This process can preserve a large part of spatial information.

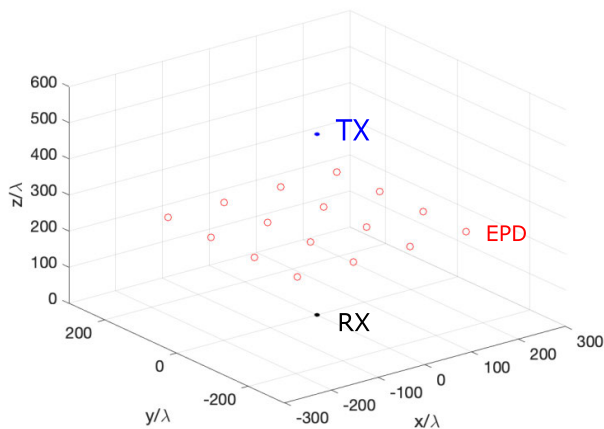


**FIGURE 9.** Geometry of the problem: the transmitting antenna is drawn in blue, the receiving antenna is drawn in black; the elements of the EPD are drawn in red.

surfaces of only  $3\lambda \times 3\lambda$ . The TX and RX antennas are placed at a distance of  $500\lambda$  and operate in free space (i.e., in the absence of the EPD, that is drawn in red in the figure).

The radiating system is simulated by a set of isotropic radiating elements placed on a  $\lambda/2$  uniform lattice. The field radiated by the transmitting elements is evaluated on the surface of the receiving antenna on a  $\lambda/2$  uniform lattice.

The matrix relating the field on the observation points to the currents on the radiating elements (i.e. whose  $(i, j)$  element is the field observed on the  $i$ -th receiving antenna radiated by the  $j$ -th transmitted antenna) is calculated and the Singular Value Decomposition is applied to the matrix. The plot of the singular values normalized to first singular value is shown in Fig. 11 as a blue curve labeled TX-RX. We can note that the singular values rapidly decay to a negligible value. In practice, only one singular value gives contribution to the capacity. Using the geometrical intuitive approach outlined in Sec. III, the set  $X$  of the currents (Fig. 10(a)) is mapped in an hyper ellipsoid  $Y$  so elongated (Fig. 10(b)) that allows packing spheres only along one dimensions. Supposing  $\epsilon = 0.2$  we have 10 distinguishable field configurations on the receiving antenna and the  $\epsilon$ -capacity turns out to be  $C_\epsilon = 3.2$  bits.

Now, let us introduce an EPD. We consider a widely distributed EPD of  $4 \times 4$  isotropic scattering objects distributed on a surface with dimension  $190\lambda \times 190\lambda$  (red points in Fig. 9).

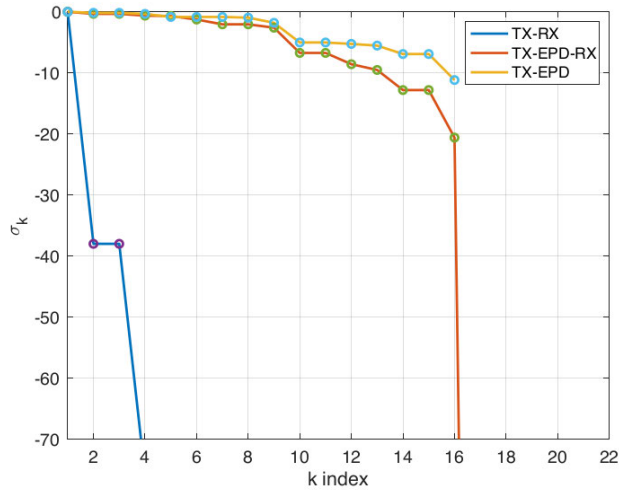


**FIGURE 11.** Normalized singular values [dB] in case of  $4 \times 4$  EPD elements; violet points: TX-RX connection in absence of EPD; red points:TX-RX connection in presence of EPD; blue points:TX-EPD connection.

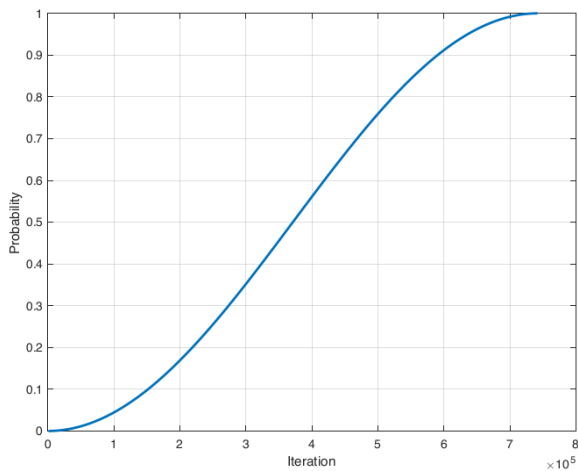


**FIGURE 12.** Probability that the wave function collapses in the goal state versus the number of iterations.

The normalized singular values of the propagation matrix relating the Transmitting elements to the EPD elements, i.e., considering the EPD as a ‘receiver,’ are plotted in Fig. 11 as blue points on yellow curve (labeled as “TX-EPD”). The number of EPD elements ( $4 \times 4$ ) limits the number of singular values of the channel operator to 16. All the 16 singular values have high amplitude, indicates that the EPD is able to collect a significant fraction of spatial information that is lost in a TX-RX direct connection. With reference to the model described in Section III, the set  $X$  (Fig. 11(d)) is mapped by the  $\mathcal{B}$  operator (Fig. 11(e)) in a 16-dimensions set  $Y_{\mathcal{B}}$  (Fig. 11(f)) having much larger volume compared to volume in absence of EPD.

The currents on the EPD (Fig. 10(g)), induced by the incident field and modified by the  $\mathcal{W}$  operator (Fig. 10(f)), radiate toward the receiving antenna (Fig. 10(h)), obtaining

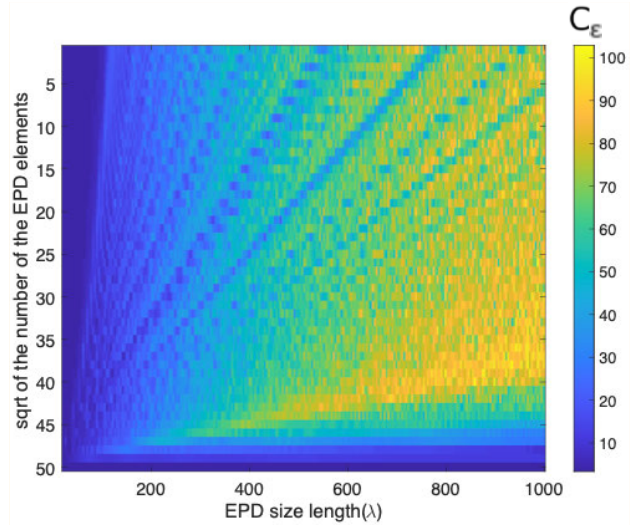


**FIGURE 13.**  $\epsilon$ -capacity [bits] versus EPD side length (measured in  $\lambda$ ) and the square root of the number of elements of the EPD. The elements of the EPD are placed on a uniform lattice.

a 16-dimensions set  $Y$  whose volume is larger compared to the absence of EPD (Fig. 10(i)). The normalized singular values of the TX-EPD-RX propagation channel are plotted as a green points on red curve in Fig. 11 (labeled TX-EPD-RX). The use of EPDs increases  $C_{\epsilon}$  from 3.2 bits in absence of EPD to 39 bits.

The Grover’s algorithm is utilized to determine the transmitted codeword.

As discussed in the previous Section, quantum algorithms give a solution in probabilistic terms. In Fig. 12, the probability that the quantum state collapses in the goal eigenstate is plotted versus the number of applications of the Grover operator (i.e., ‘iterations’ of the quantum algorithm’). We can note that the algorithm gives the “correct” eigenstate with unit probability in about 750.000 iterations, while a search using nonquantum computers would require on average more than 250 billion trials to identify the transmitted codeword.

This example gives only a limited idea of the potentialities present in the DPL. Several optimization can be carried out. Fig. 13 shows  $C_{\epsilon}$  versus the length of the side of the EPD and the square root of the number of radiating elements, indicating that it is possible further significant increase of the capacity at least up to 100 bits.

The examples suggest huge potential in DPL, which can be fully exploited using EPDs and quantum computing.

## VI. CONCLUSION

This work explores the potential of leveraging field processing in the Deep Physical Layer (DPL) to enhance the amount of information that can be transmitted via wireless communication systems. The analysis is divided into two parts, the first of which focuses on Electromagnetic Processing Devices (EPDs), which operate on classical physics principles. By acting as “lenses,” EPDs gather information from large areas

of space that would have otherwise been lost and make it available to the receiver.

The “information lenses” of EPDs share several similarities with RIS. EPDs can be viewed as an optimized configuration of reflecting surfaces that maximizes channel capacity. In this sense, an EPD is to a RIS what a transmitting array [51] is to a single element of the array.

The amount of information that can be encoded in space can be extremely large. The quantitative improvement depends of a number of factors (antennas, propagation environment, frequency, design of the EPD) and can reach, at least in theory, over 100 bits per symbol. This makes identifying the code word associated with the a set of field configurations belonging to optimal sphere packing challenging to handle with classical computers. The second part of the elaboration exploits quantum computing to fulfill this role.

This work’s findings indicate that quantum computers are a vital technology to obtain unrestricted access to the large resources that the utilization of EPDs can unlock at the DPL.

The feasibility of the concepts discussed in this paper is supported by experimental evidence of improved channel capacity through the use of controlled reflecting element arrays [27].

Implementation of static EPDs is indeed already possible. Regarding the applications of EPD, while the primary challenge of millimeter wave systems lies in extending coverage to non-line-of-sight areas, the key issue for lower frequency systems is enhancing the system’s capacity in terms of bit rate and the number of users served. Consequently, lower frequency systems below 6 GHz would reap greater benefits.

The primary challenge to widespread adoption is cost reduction. One possible solution is to leverage technological advancements in the related field of reconfigurable intelligent surfaces (RIS), such as the development of new materials like graphene [52], [53], which can also be applied to EPDs.

Regarding the exploitation of quantum computing, we must note that the bright future promised by enthusiasts presents shadow spots raised by doubts about the limits of the quantum approach [54].

Quantum computers are basically probabilistic Turing machines that make a random choice between multiple possible dynamical evolutions. Consequently, they cannot compute a function that is not computable by a deterministic Turing machines. The different is given by the efficiency of the computation, that for some classes of problems is higher in case of quantum computers.

It is probable that the application of quantum computers will be restricted to specific tasks where the quantum superposition provides an advantage over classical parallel computing solutions. The present paper proposes an approach that combines classical and quantum processing, which aligns with this view. Oracles play a critical role as the link between the classical and quantum worlds. Their optimization has a significant impact on the overall computational efficiency of

such systems, and their optimization deserves the attention of quantum computing researchers.

Implementation of Grover’s algorithm for the application discussed in this paper appears to be feasible in the close future. The  $\epsilon$ -capacity of spatial channels for the examples discussed in this paper ranges from a few tens of bits to around one hundred, making the required number of qubits manageable. In the literature, there are examples of implementing Grover’s algorithm on actual quantum computers with a small number of qubits since 2017 [55]. Furthermore, as of 2022, a 433-qubit quantum processor (IBM Osprey) is currently operational, and by the end of 2025, IBM Quantum System 2 is expected to have over 4000 qubits.

However, the scalability of the Grover algorithm is not a straightforward task as it depends not only on the number of qubits but also on their quality, which is limited by the decoherence phenomenon. Additionally, implementing the oracle also has a significant impact on the actual implementation of the Grover’s algorithm.

In order to analyze classical and quantum mixed systems, it is necessary to have a consistent mathematical framework. In this paper, a considerable effort has been made to achieve such a framework both mathematically and conceptually, by using operators to describe the transformations of the electromagnetic field, which is of interest in the classical world, and qubits in the quantum world.

Viewed from this unified mathematical perspective, the proposed method can be summarized quite simply. It capitalizes on the fact that classical fields do not collapse into a single singular function, generating a large number of distinguishable field states at the receiver, each corresponding to a different code word. Additionally, it leverages the fact that the quantum wave function represents a superposition of all eigenstates simultaneously, enabling rapid identification of the transmitted code word.

In conclusion, this article examines the fundamental concept of EPDs and presents some numerical results on static EPDs. Dynamic EPDs, for which higher potential performance is expect, will be object of research in the future. This article also explores the combination of classical and quantum physics in communication. One critical consideration is where to draw the boundary between classical and quantum systems in practical applications. In this paper this boundary is placed at the signal’s reception with quantum systems solely used for optimal receiving. However, there is potential to shift this boundary by incorporating quantum sensing in signal reception or leveraging entanglement in information transmission. The fusion of classical and quantum computing represents an exciting new frontier in research.

#### APPENDIX. A SIMPLE EXAMPLE OF IMPLEMENTATION OF GROVER’S ALGORITHM

To give a simple example of how the GQSA can be implemented in quantum computers, suppose that  $C_\epsilon = 2$ , i.e.,  $N = 4$ , and the received signal belongs to the  $\epsilon$ -sphere whose

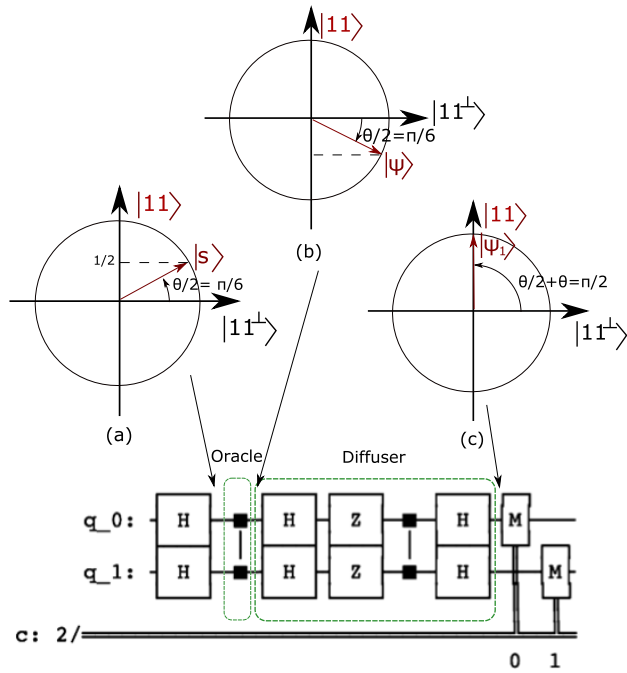


**FIGURE 14.** Grover algorithm in case of  $|11\rangle$  goal state. Upper figure: steps of the algorithm. Lower figure: implementation using quantum gates. H is the Hadamard gate. The Controlled-Z gate (CZGate) is represented by the two small dots connected by a vertical line. Z is the Z gate. M is measurement circuit. The quantum circuit has been obtained using Quiskit Grover class [56].

index is  $k = 3$ . The 4 possible  $\epsilon$ -spheres are encoded in 4 eigenstates:  $|00\rangle, |01\rangle, |10\rangle, |11\rangle$ . The goal state is  $|11\rangle$ .

The state at beginning of the procedure is (Fig. 14 (a)) [33]:

$$|s\rangle = \left(\frac{|0\rangle + |1\rangle}{\sqrt{2}}\right) \otimes \left(\frac{|0\rangle + |1\rangle}{\sqrt{2}}\right) = \frac{1}{2}(|00\rangle + |01\rangle + |10\rangle + |11\rangle)$$

(wherein  $\otimes$  is the Kronecker product), while  $|11^\perp\rangle$ , given by the superposition of all the eigenstates but the goal eigenstate, is:

$$|11^\perp\rangle = \frac{1}{\sqrt{3}}(|00\rangle + |01\rangle + |10\rangle)$$

With reference to Fig. 14 (a), the projection of  $|s\rangle$  onto the goal state  $|11\rangle$  is  $1/2$ , and the angle  $\theta/2$  is equal to  $\pi/6$ . The probability that the  $|s\rangle$  collapses in  $|11\rangle$  is the square of the projection, i.e.  $1/4$ .

Application of the oracle operator gives (Fig. 14 (b)) [33]:

$$|\psi\rangle = U_{11} |s\rangle = \frac{1}{2}(|00\rangle + |01\rangle + |10\rangle - |11\rangle)$$

Finally, application of the diffusion operator rotates  $|\psi\rangle$  of  $2\theta$ . Consequently, the angle of  $|\psi_1\rangle$  is  $\pi/6 + \pi/3 = \pi/2$ , and the superposition of states collapses in  $|11\rangle$  in only one step with 100% probability (Fig. 14 (c)).

Quantum gates admit a representation in terms of unitary matrices, while the states  $|00\rangle, |01\rangle, |10\rangle$  and  $|11\rangle$  are represented in terms of column vectors  $[1000]^T, [0100]^T, [0010]^T,$

**TABLE 3.** Truth table of quantum gates involved in the Grover's circuit and matrix representation of the gate [57].

Gate	Input	Output	Matrix representation
Z gate	$ 0\rangle$ $ 1\rangle$	$ 0\rangle$ $- 1\rangle$	$\begin{bmatrix} 1 & 0 \\ 0 & -1 \end{bmatrix}$
Hadamard	$ 0\rangle$ $ 1\rangle$	$\frac{ 0\rangle+ 1\rangle}{\sqrt{2}}$ $\frac{ 0\rangle- 1\rangle}{\sqrt{2}}$	$\frac{1}{\sqrt{2}} \begin{bmatrix} 1 & 1 \\ 1 & -1 \end{bmatrix}$
CZ-gate	$ 00\rangle$ $ 01\rangle$ $ 10\rangle$ $ 11\rangle$	$ 00\rangle$ $ 01\rangle$ $ 10\rangle$ $- 11\rangle$	$\begin{bmatrix} 1 & 0 & 0 & 0 \\ 0 & 1 & 0 & 0 \\ 0 & 0 & 1 & 0 \\ 0 & 0 & 0 & -1 \end{bmatrix}$

$[0001]^T$ , where the superscript  $T$  stands for the transpose of the vector. Consequently,  $n$  qubits are associated to  $N = 2^n$ -entries vectors.

Fig. 14 (lower figure) shows the quantum circuit implementing the algorithm above outlined. The circuit involves three different quantum gates [57] (see Table 3): the Hadamard gate (H), the Z gate and the Controlled-Z gate, that applies a Z-gate to the second qubit if the first qubit is in the state  $|1\rangle$ .

The system is posed in a uniform state superposition using Hadamard gates, that transform the pure  $|00\rangle$  state

$$a_0 = \begin{bmatrix} 1 \\ 0 \\ 0 \\ 0 \end{bmatrix}$$

in the uniformly mixed state [57]

$$a_1 = (H \otimes H) a_0 = \frac{1}{2} \begin{bmatrix} 1 \\ 1 \\ 1 \\ 1 \end{bmatrix}$$

The oracol operator  $U_{11}$ :

$$U_{11} = \begin{bmatrix} 1 & 0 & 0 & 0 \\ 0 & 1 & 0 & 0 \\ 0 & 0 & 1 & 0 \\ 0 & 0 & 0 & -1 \end{bmatrix}$$

is implemented by a Controlled-Z Gate [57], obtaining:

$$a_2 = (CZ) a_1 = \frac{1}{2} \begin{bmatrix} 1 \\ 1 \\ 1 \\ -1 \end{bmatrix}$$

The diffuser s implemented by an Hadamard gate followed by a Z-gate, a Controlled zeta gate and a Hadarad gate, obtaining the goal state:

$$a_3 = (H \otimes H)(CZ)(Z \otimes Z)(H \otimes H) = \begin{bmatrix} 0 \\ 0 \\ 0 \\ 1 \end{bmatrix}$$

The circuit is described in many books and in the Quiskit web site [56], [57], to which the interested reader can refer to obtain detailed information on the circuit. The algorithm can also be executed on real quantum computers [36].



## ACKNOWLEDGMENT

Views and opinions expressed are, however, those of the authors only and do not necessarily reflect those of the European Union. Neither the European Union nor the granting authority can be held responsible for them.

## REFERENCES

- [1] C. E. Shannon, "A mathematical theory of communication," *Bell Syst. Tech. J.*, vol. 27, no. 3, pp. 379–423, Jul./Oct. 1948.
- [2] R. Piestun and D. A. B. Miller, "Electromagnetic degrees of freedom of an optical system," *J. Opt. Soc. Amer. A, Opt. Image Sci.*, vol. 17, no. 5, pp. 892–902, 2000.
- [3] J. W. Wallace and M. A. Jensen, "Intrinsic capacity of the MIMO wireless channel," in *Proc. IEEE 56th Veh. Technol. Conf.*, vol. 2, Sep. 2002, pp. 701–705.
- [4] S. Loyka, "Information theory and electromagnetism: Are they related?" in *Proc. 10th Int. Symp. Antenna Technol. Appl. Electromagn. URSI Conf.*, Jul. 2004, pp. 1–5.
- [5] T. K. Sarkar, S. Burintramart, N. Yilmazer, S. Hwang, Y. Zhang, A. De, and M. Salazar-Palma, "A discussion about some of the principles/practices of wireless communication under a Maxwellian framework," *IEEE Trans. Antennas Propag.*, vol. 54, no. 12, pp. 3727–3745, Dec. 2006.
- [6] M. D. Migliore, "Restoring the symmetry between space domain and time domain in the channel capacity of MIMO communication systems," in *Proc. IEEE Antennas Propag. Soc. Int. Symp.*, Jul. 2006, pp. 333–336.
- [7] M. D. Migliore, "On the role of the number of degrees of freedom of the field in MIMO channels," *IEEE Trans. Antennas Propag.*, vol. 54, no. 2, pp. 620–628, Feb. 2006.
- [8] J. Xu and R. Janaswamy, "Electromagnetic degrees of freedom in 2-D scattering environments," *IEEE Trans. Antennas Propag.*, vol. 54, no. 12, pp. 3882–3894, Dec. 2006.
- [9] A. S. Y. Poon, R. W. Brodersen, and D. N. C. Tse, "Degrees of freedom in multiple-antenna channels: A signal space approach," *IEEE Trans. Inf. Theory*, vol. 51, no. 2, pp. 523–536, Feb. 2005.
- [10] M. Gustafsson and S. Nordebo, "Characterization of MIMO antennas using spherical vector waves," *IEEE Trans. Antennas Propag.*, vol. 54, no. 9, pp. 2679–2682, Sep. 2006.
- [11] A. Poon and D. Tse, "Polarization degrees of freedom," in *Proc. IEEE Int. Symp. Inf. Theory*, Jul. 2008, pp. 1587–1591.
- [12] F. K. Gruber and E. A. Marengo, "New aspects of electromagnetic information theory for wireless and antenna systems," *IEEE Trans. Antennas Propag.*, vol. 56, no. 11, pp. 3470–3484, Nov. 2008.
- [13] M. Franceschetti, M. D. Migliore, and P. Minero, "The capacity of wireless networks: Information-theoretic and physical limits," *IEEE Trans. Inf. Theory*, vol. 55, no. 8, pp. 3413–3424, Aug. 2009.
- [14] M. Franceschetti, M. D. Migliore, P. Minero, and F. Schettino, "The information carried by scattered waves: Near-field and nonasymptotic regimes," *IEEE Trans. Antennas Propag.*, vol. 63, no. 7, pp. 3144–3157, Jul. 2015.
- [15] M. D. Migliore, "On electromagnetics and information theory," *IEEE Trans. Antennas Propag.*, vol. 56, no. 10, pp. 3188–3200, Oct. 2008.
- [16] M. D. Migliore, "Horse (electromagnetics) is more important than horse-man (information) for wireless transmission," *IEEE Trans. Antennas Propag.*, vol. 67, no. 4, pp. 2046–2055, Apr. 2019.
- [17] M. D. Migliore, "Who cares about the horse? A gentle introduction to information in electromagnetic theory [wireless corner]," *IEEE Antennas Propag. Mag.*, vol. 62, no. 5, pp. 126–137, Oct. 2020.
- [18] D. Pinchera, M. Lucido, G. Chirico, F. Schettino, and M. D. Migliore, "Controllable local propagation environment to maximize the multiplexing capability of massive MIMO systems," *Electronics*, vol. 12, no. 9, p. 2022, Apr. 2023. [Online]. Available: <https://www.mdpi.com/2079-9292/12/9/2022>
- [19] A. Pizzo, T. L. Marzetta, and L. Sanguinetti, "Degrees of freedom of holographic MIMO channels," 2019, *arXiv:1911.07516*.
- [20] A. Pizzo, A. D. J. Torres, L. Sanguinetti, and T. L. Marzetta, "Nyquist sampling and degrees of freedom of electromagnetic fields," *IEEE Trans. Signal Process.*, vol. 70, pp. 3935–3947, 2022.
- [21] Z. Wan, J. Zhu, Z. Zhang, L. Dai, and C. Chae, "Mutual information for electromagnetic information theory based on random fields," *IEEE Trans. Commun.*, vol. 71, no. 4, pp. 1982–1996, Apr. 2023.
- [22] M. D. Migliore, "The world beneath the physical layer: An introduction to the deep physical layer," *IEEE Access*, vol. 9, pp. 77106–77126, 2021.
- [23] D. Pinchera, M. D. Migliore, and F. Schettino, "Optimizing antenna arrays for spatial multiplexing: Towards 6G systems," *IEEE Access*, vol. 9, pp. 53276–53291, 2021.
- [24] M. D. Migliore, "Information flows at the deep physical layer level," in *A Glimpse Beyond 5G in Wireless Networks*. New York, NY, USA: Springer, 2022, pp. 59–87.
- [25] Video. (2022). *Electromagnetic Field Processing at the Deep Physical Layer Level*. Accessed: Mar. 18, 2023. [Online]. Available: <https://youtu.be/va5JojlUPP4>
- [26] M. D. Migliore, D. Pinchera, and F. Schettino, "Improving channel capacity using adaptive MIMO antennas," *IEEE Trans. Antennas Propag.*, vol. 54, no. 11, pp. 3481–3489, Nov. 2006.
- [27] D. Pinchera, J. W. Wallace, M. D. Migliore, and M. A. Jensen, "Experimental analysis of a wideband adaptive-MIMO antenna," *IEEE Trans. Antennas Propag.*, vol. 56, no. 3, pp. 908–913, Mar. 2008.
- [28] P. Rocca, P. D. Rù, N. Anselmi, M. Salucci, G. Oliveri, D. Erricolo, and A. Massa, "On the design of modular reflecting EM skins for enhanced urban wireless coverage," *IEEE Trans. Antennas Propag.*, vol. 70, no. 10, pp. 8771–8784, Oct. 2022.
- [29] E. Basar, M. Di Renzo, J. De Rosny, M. Debbah, M.-S. Alouini, and R. Zhang, "Wireless communications through reconfigurable intelligent surfaces," *IEEE Access*, vol. 7, pp. 116753–116773, 2019.
- [30] E. Martini and S. Maci, "Theory, analysis, and design of metasurfaces for smart radio environments," *Proc. IEEE*, vol. 110, no. 9, pp. 1227–1243, Sep. 2022.
- [31] Y. Liu, X. Liu, X. Mu, T. Hou, J. Xu, M. Di Renzo, and N. Al-Dhahir, "Reconfigurable intelligent surfaces: Principles and opportunities," *IEEE Commun. Surveys Tuts.*, vol. 23, no. 3, pp. 1546–1577, 3rd Quart., 2021.
- [32] S. Basharat, S. A. Hassan, H. Pervaiz, A. Mahmood, Z. Ding, and M. Gidlund, "Reconfigurable intelligent surfaces: Potentials, applications, and challenges for 6G wireless networks," *IEEE Wireless Commun.*, vol. 28, no. 6, pp. 184–191, Dec. 2021.
- [33] E. Desurvire, *Classical and Quantum Information Theory: An Introduction for the Telecom Scientist*. Cambridge, U.K.: Cambridge Univ. Press, 2009.
- [34] N. P. de Leon, K. M. Itoh, D. Kim, K. K. Mehta, T. E. Northup, H. Paik, B. S. Palmer, N. Samarth, S. Sangtawesin, and D. W. Steuerman, "Materials challenges and opportunities for quantum computing hardware," *Science*, vol. 372, no. 6539, Apr. 2021, Art. no. eabb2823.
- [35] F. T. Chong, D. Franklin, and M. Martonosi, "Programming languages and compiler design for realistic quantum hardware," *Nature*, vol. 549, no. 7671, pp. 180–187, Sep. 2017.
- [36] (2023). *Quantum Computing*. Accessed: Mar. 18, 2023. [Online]. Available: <https://quantum-computing.ibm.com/>
- [37] A. Kolmogorov and S. Fomin, *Elements of the Theory of Functions and Functional Analysis*. New York, NY, USA: Dover, 1999.
- [38] D. S. Jones, *Acoustic and Electromagnetic Waves*. New York, NY, USA: Oxford, 1986.
- [39] G. W. Hanson and A. B. Yakovlev, *Operator theory for Electromagnetics: An Introduction*. New York, NY, USA: Springer, 2013.
- [40] V. Tikhomirov, " $\varepsilon$ -entropy and  $\varepsilon$ -capacity of sets in functional spaces," in *Selected Works of A. N. Kolmogorov*. New York, NY, USA: Springer, 1993, pp. 86–170.
- [41] R. T. Prosser and W. L. Root, "The  $\varepsilon$ -entropy and  $\varepsilon$ -capacity of certain time-invariant channels," *J. Math. Anal. Appl.*, vol. 21, no. 2, pp. 233–241, 1968.
- [42] O. M. Bucci and G. Franceschetti, "On the degrees of freedom of scattered fields," *IEEE Trans. Antennas Propag.*, vol. 37, no. 7, pp. 918–926, Jul. 1989.
- [43] O. M. Bucci, C. Gennarelli, and C. Savarese, "Representation of electromagnetic fields over arbitrary surfaces by a finite and nonredundant number of samples," *IEEE Trans. Antennas Propag.*, vol. 46, no. 3, pp. 351–359, Mar. 1998.
- [44] M. D. Migliore, D. Franci, S. Pavoncello, T. Aureli, E. Merli, C. Lodovisi, L. Chiaraviglio, and F. Schettino, "Application of the maximum power extrapolation procedure for human exposure assessment to 5G millimeter waves: Challenges and possible solutions," *IEEE Access*, vol. 10, pp. 103438–103446, 2022.
- [45] M. Di Renzo and S. Tretyakov, "Reconfigurable intelligent surfaces," *Proc. IEEE*, vol. 110, no. 9, pp. 1159–1163, Sep. 2022.

- [46] L. K. Grover, "A fast quantum mechanical algorithm for database search," in *Proc. 28th Annu. ACM Symp. Theory Comput.*, 1996, pp. 212–219.
- [47] C. Zalka, "Grover's quantum searching algorithm is optimal," *Phys. Rev. A, Gen. Phys.*, vol. 60, no. 4, p. 2746, 1999.
- [48] L. K. Grover, "Quantum mechanics helps in searching for a needle in a haystack," *Phys. Rev. Lett.*, vol. 79, no. 2, pp. 325–328, Jul. 1997.
- [49] G. Brassard, P. Hoyer, M. Mosca, and A. Tapp, "Quantum amplitude amplification and estimation," *Contemp. Math.*, vol. 305, pp. 53–74, Oct. 2002.
- [50] M. D. Migliore, "Big, bigger, biggest. What should we expect from 6G antennas?" in *Proc. XXXIII Gen. Assem. Sci. Symp. Int. Union Radio Sci.*, Aug. 2020, pp. 1–4.
- [51] D. Berry, R. Malech, and W. Kennedy, "The reflectarray antenna," *IEEE Trans. Antennas Propag.*, vol. AP-11, no. 6, pp. 645–651, Nov. 1963.
- [52] T. J. Cui, "Microwave metamaterials—From passive to digital and programmable controls of electromagnetic waves," *J. Opt.*, vol. 19, no. 8, Aug. 2017, Art. no. 084004.
- [53] M. Lucido, F. Schettino, and G. Panariello, "Scattering from a thin resistive disk: A guaranteed fast convergence technique," *IEEE Trans. Antennas Propag.*, vol. 69, no. 1, pp. 387–396, Jan. 2021.
- [54] S. Aaronson, "The limits of quantum," *Sci. Amer.*, vol. 298, no. 3, pp. 62–69, 2008.
- [55] C. Figgatt, D. Maslov, K. A. Landsman, N. M. Linke, S. Debnath, and C. Monroe, "Complete 3-qubit Grover search on a programmable quantum computer," *Nature Commun.*, vol. 8, no. 1, p. 1918, Dec. 2017.
- [56] Quiskit. (2023). *Grover Algorithm*. Accessed: Mar. 18, 2023. [Online]. Available: <https://qiskit.org/textbook/ch-algorithms/grover.html>
- [57] M. Coggins, *Introduction to Quantum Computing With Qiskit*. Scarborough, U.K.: Scarborough Quantum Computing, 2021.



**MARCO DONALD MIGLIORE** (Senior Member, IEEE) received the Laurea (Hons.) and Ph.D. degrees in electronic engineering from the University of Naples, Naples, Italy. He was a Visiting Professor with the University of California at San Diego, La Jolla, CA, USA, in 2007, 2008, and 2017, the University of Rennes I, Rennes, France, in 2014 and 2016, the Centria Research Center, Ylivienka, Finland, in 2017, the University of Brasilia, Brazil, in 2018, and Harbin Technical University, China, in 2019. He is currently a Full Professor with the University of Cassino and Southern Lazio, Cassino, Italy, where he is also the Head of the Microwave Laboratory and the Director of Studies of the ITC courses. He is also a member of the ELEDIA@UniCAS Research Laboratory, National Interuniversity Research Center on the Interactions between Electromagnetic Fields and Biosystems (ICEMmB), where he is also the Leader of the 5G Group, Italian Electromagnetic Society (SIEM), and the National Interuniversity Consortium for Telecommunication (CNIT). His current research interests include the connections between electromagnetism and information theory, analysis, synthesis and characterization of antennas in complex environments, antennas and propagation for 5G, *ad-hoc* wireless networks, compressed sensing as applied to electromagnetic problems, energetic applications of microwaves, fusion between classical, and quantum processing. He was a Speaker at the Summer Research Lecture Series of the UCSD CALIT2 Advanced Network Science, in 2008. He serves as a referee for many scientific journals. He has served as an Associate Editor for IEEE TRANSACTIONS ON ANTENNAS AND PROPAGATION.

• • •